

## Kinetic modeling of an anaerobic fixed-bed reactor treating industrial wastewater containing hydrothermally solubilized sugarcane bagasse and post-treatment evaluation

Bing Liu<sup>a,b</sup>, Anh Van Ngo<sup>c</sup>, Meng Sun<sup>b</sup>, Jing Wang<sup>a</sup>, Nguyen The Anh<sup>b</sup>, Mitsuharu Terashima<sup>b,\*</sup>, Hidenari Yasui<sup>b</sup>

<sup>a</sup>Resources and Environment Innovation Research Institute, School of Municipal and Environmental Engineering, Shandong Jianzhu University, Jinan 250101, Shandong, China, Tel. +86-531-8636-1857; emails: b-liu@sdjzu.edu.cn (B. Liu), jwang@sdjzu.edu.cn (J. Wang)

<sup>b</sup>Graduate School of Environmental Engineering, The University of Kitakyushu, 1-1 Hibikino, Wakamatsu, Kitakyushu, Fukuoka 8080135, Japan, Tel. +81-93-695-3212; email: m-terashima@kitakyu-u.ac.jp (M. Terashima), Tel. +81-93-695-3736; emails: y7dac404@eng.kitakyu-u.ac.jp (M. Sun), y7dac002@eng.kitakyu-u.ac.jp (N. The Anh), hidenari-yasui@kitakyu-u.ac.jp (H. Yasui)

<sup>c</sup>Department of Environmental Technology, VNU University of Science, 334 Nguen Trai Street, Thanh Xuan District, Hanoi 10000, Vietnam, Tel. +81-93-695-3736; email: ngovananh3012@gmail.com (A. Van Ngo)

Received 13 May 2019; Accepted 19 March 2020

### ABSTRACT

Bioethanol has emerged as a major alternative and environment-friendly fuel to face with energy consumption increasing in recent decades. In bioethanol processing factories, new technologies using steam explosion pretreatments are developed to improve ethanol production from cellulose (e.g. sugarcane bagasse). However, wastewater from this step with high chemical oxygen demand (COD), high soluble total organic carbon (S-TOC), low pH, and dark brown color cause serious environmental problems. This research focused on the high-rate anaerobic wastewater treatment from bioethanol production using a fixed-bed reactor. A 10.8 L lab-scale reactor was continuously operated at 35°C for 160 d with a volumetric loading rate of 10.9 kg-COD/m<sup>3</sup>/d. A kinetic model based on a modification of anaerobic digestion model no. 1 and activated sludge models was used to reasonably simulate the methane production, soluble TOC, suspended solid as well as the soluble effluent constituents in terms of carbohydrate, protein, propionate, acetate, lignin, and ammonium nitrogen. The steady-state simulation results showed that 45% of COD was converted to methane with a high organic loading rate (9.72 kg-COD/m<sup>3</sup>/d). In addition, tests using physicochemical methods were conducted to remove un-biodegradable materials and color from the effluent. Oxidation, coagulation/flocculation, and adsorption removed 88% of soluble TOC and 98% of color.

*Keywords:* Anaerobic; Fixed-bed reactor; Kinetic model; Steam explosion wastewater

### 1. Introduction

With the development of science and technology, it is one of the most promising biomass fractionation processes to produce bioethanol from lignocellulosic materials by the steam explosion [1–4]. Among the various feedstock

sources, sugarcane bagasse is the most potential resource [5,6]. Pretreatment of bagasse by the steam explosion can replace or eliminate the structural and compositional hindrance to hydrolysis and increase the yield of fermentable sugar from cellulose or hemicellulose [7–9]. However, the great challenge for the production of bioethanol by the steam explosion is how to use all kinds of the waste left in

\* Corresponding author.

the production process, reduce the impact on the environment, and effectively use energy. Most of the liquid residuals have high organic strength and nutrients, for instance, more than 20 g-COD/L, and high nutrients content, more than 100 mg-N/L and more than 25 mg-P/L containing [10,11], which is fit for anaerobic methane fermentation process due to unpowered requirement and energy production (methane). Therefore, the wastewater of the steam explosion process might be a source of biogas production or recovery [12]. An up-flow anaerobic sludge blanket (UASB) granule reactor and mesophilic two-stage anaerobic digestion process were utilized to treat steam explosion wastewater (SEWW) for methane fermentation [11,13]. Anyway, there are still some places that need to be improved due to the poor effluent quality in previous researches [11,14,15]. In other words, in wastewater from the steam explosion process, the conditions of low pH (inhibitor factor for biological reaction) [16], un-biodegradable material (for instance lignin), and accumulated organic acid (inhibitor for the process) were difficult in the anaerobic fermentation process [17]. Additionally, the treatment of effluent from the anaerobic process was another difficulty in the whole treatment process [18].

High-rate anaerobic treatment processes are rapidly becoming popular for industrial wastewater treatment. The advantages of the process are low energy consumption, short hydraulic retention times (HRTs), and high organic loading rates (OLRs) [19,20]. The technologies applying high-rate anaerobic digestion include fixed-bed reactors (FBR), UASB, moving-bed biofilm reactor, expanded granular sludge beds, sequencing batch reactors, and anaerobic hybrid/hybrid UASB reactors [20]. The biomass of the FBR system can retain and attach to the support materials and help avoid the loss of biomass from the reactor [21]. At the same time, the process is very stable and resistant to stress such as overloading of organic or changes in pH and temperature [22–24].

This research focused on the experimental investigation of the high-rate anaerobic treatment of wastewater from the bioethanol production process over a period of 5 months using an FBR, which is the first report for wastewater

treatment from steam explosion process using FBR according to published research reports. To express the reactor performances in a mathematical manner, a kinetic model was developed based on a modification of anaerobic digestion model no 1 (ADM1) [25] and activated sludge models (ASMs) [26]. Additionally, in an effort to remove the total organic carbon and color from the effluent of the FBR, oxidation combining coagulation using NaClO and polyaluminum chloride (PAC) [27], and nanofiltration (NF) and reverse osmosis membrane (RO) post-treatment were conducted in this study.

## 2. Materials and methods

To clearly describe test contents and methods in each step of this study, the research and experimental flow was listed and shown in Fig. 1.

### 2.1. Analytical procedures and composition of the SEWW

Total solids, suspended solids (SS), total volatile solids, chemical oxygen demand (COD), soluble total organic carbon (S-TOC), total nitrogen, ammonium nitrogen, total phosphorus, and inorganic cations concentrations, respectively were measured according to #2540 B, D, E, #5220 D, #5310 B, #4500-N B, #4500-NH<sub>3</sub> F, #4500-P E and 3120-B in Standard Methods [28]. Soluble carbohydrate, protein, lignin furfural, hydroxyl-methyl-furfural, fatty acid, inorganic cation and anion concentrations, the composition of sugars were measured according to the reference methods [11,29,30].

The steam-explosion of sugarcane bagasse collected was carried out under 3.0 MPa for 5 min at about 230°C followed by instantaneous depressurization to ambient pressure. The solid product was washed with tap water as much as 5 times the bulk volume of the bagasse material before filtration, and the SEWW (liquid fraction) was separated from the composite accordingly [11,15]. The 3 times' collected SEWW samples used for the influent of continuous anaerobic digestion experiment, the above analysis methods were utilized for SEWW.

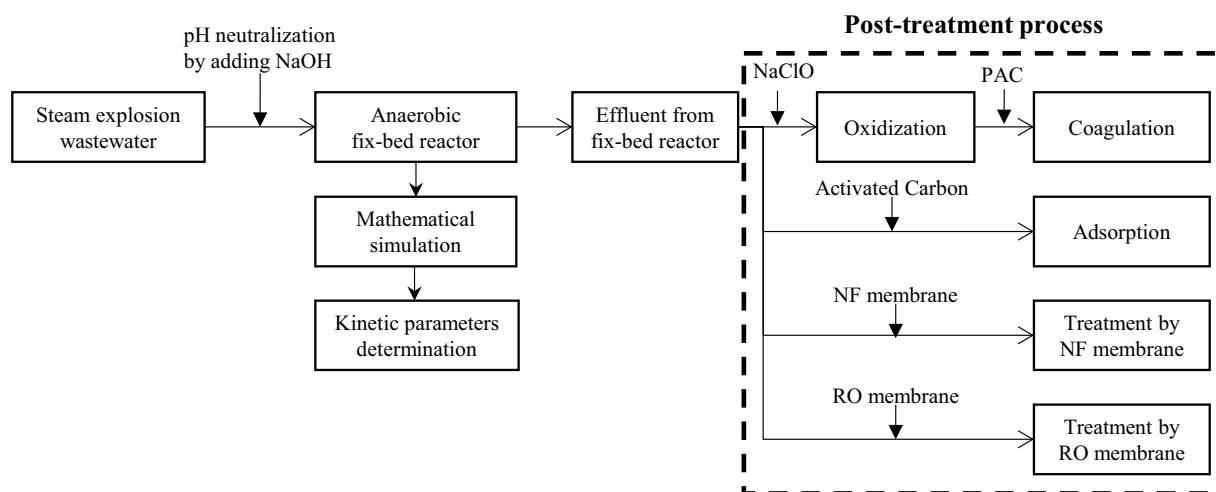


Fig. 1. The research and experimental flow in this study.

## 2.2. Continuous experiment reactor

A lab-scale continuous fixed-bed anaerobic reactor (filled with short plastic media of 10 mm height and 8 mm diameter corresponding to 350 m<sup>2</sup>-carrier surface/m<sup>3</sup>-reactor) was operated at 35°C ± 2°C with a working volume of 10.8 L (Fig. 2). For the fixed-bed anaerobic process, 5 L seed anaerobic sludge was collected from a mesophilic digester at Hiagari Municipal Wastewater Treatment Plant, Kitakyushu, Japan operated at about 38 d HRT receiving a mixture of primary and secondary sludge from a conventional biochemical oxygen demand removal activated sludge process. Seed anaerobic sludge was pumped into the fixed-bed anaerobic reactor for SEWW treatment, the most of seed sludge was attached in the reactor while the redundant was washed out. Since the wastewater from washing process after the steam explosion was highly acidic, NaOH 1 mol/L and a pH pump (EWN-W, IWAKI Co., Ltd., Japan) were used to neutralize the pH in the reactor (Fig. 2) and kept pH at 6.95–7.05 during whole operation period since the biological optimum pH is in neutral range while the volumetric loading rate (VLR) was increased from 4.46 to 10.94 kg-COD/m<sup>3</sup>/d in a step-wise manner. The methane gas production rate (MPR) in the reactor was continuously logged using a wet gas meter (Shinagawa Corporation, Japan).

## 2.3. Dynamic simulation

Dynamic simulation of the FBR was performed focusing on responses of methane production, soluble TOC, SS as well as the soluble effluent constituents in terms of carbohydrate, protein, propionate, acetate, lignin and ammonium nitrogen. For simulating the reactor performances and biological degradability of the wastewater organics in a mathematical manner, a kinetic model was developed based on a modification of ADM1 and ASMs. Although ADM1 and ASMs were initially referred to model the set of reactions, the individual process expressions were considerably modified in order to include the fates of furfural, hydroxymethylfurfural (HMF), lactate and formate. An anaerobic biological reaction map for the SEWW organics is shown in Fig. 3. Considering the

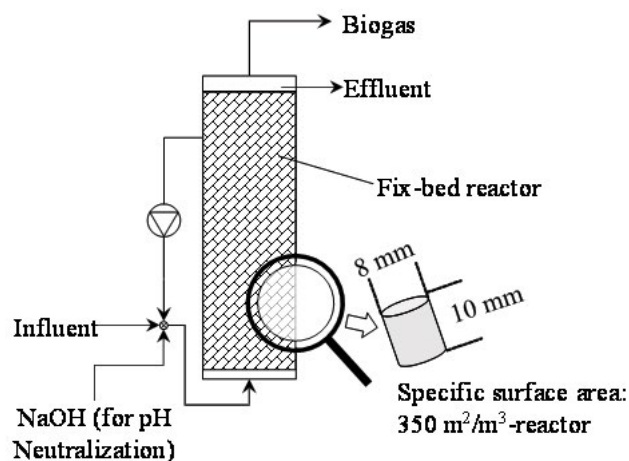


Fig. 2. Fixed-bed reactor (FBR).

soluble nature of organics in SEWW, the process map included hydrolysis ( $r1-r2$ ), acidogenesis ( $r3-r7$ ), acetogenesis ( $r8$ ), methanogenesis ( $r9-r11$ ) and decay ( $r12-r16$ ). Monosaccharide, furfural, HMF, and lactate were classified as carbohydrate species while formate and hydrogen were degraded by the hydrogenotrophic methanogen. The decayed products were defined to be carbohydrate, protein, and un-biodegradable particulate, which was an analogy of ASM3. As shown in Table 1, a Contois type (from ASMs), a Monod type, and a first-order type (from ADM1) were applied to express the reaction rates. In addition, a non-competitive inhibition function was added for hydrogen inhibition on propionate degradation. Although diffusion resistance of soluble substrates in the biofilm was not incorporated in the model, by applying high half-saturation coefficients ( $K_s$ ) of process rates the impact of biofilm on organic digestion performance was considered. Kinetics for individual organics in SEWW were estimated from simulation results of the batch biological experiment, which was conducted by mixing anaerobic sludge from a lab-scale continuous FBR and SEWW. Based on the MPR response, the degradation of organics in SEWW as well as the production of intermediates, kinetic parameters were estimated.

As the material balance of the model was COD based, COD/TOC factors were prepared to calculate the composite materials (carbohydrate, protein, and lignin) as 2.67, 3.00, and 2.92, assuming the elemental compositions (CH<sub>2</sub>O)<sub>n</sub>, (C<sub>4</sub>H<sub>9</sub>O<sub>2</sub>N)<sub>n</sub> [31] and (C<sub>31</sub>H<sub>34</sub>O<sub>11</sub>)<sub>n</sub> [32], respectively. The system responses were simulated using GPS-X Version 6.4 (Hydromantis Environmental Software Solutions, Inc., Canada). The 5 kinds of active biomass sugar degrader, amino acid degrader, propionate degrader, and acetate degrader were defined as shown in Table 2. Biomass concentrations were estimated from the yield coefficients in the literature [25] and the decrement of soluble organic concentration between the influent and effluent in continuous operation fed the wastewater [33].

## 2.4. Post-treatment for effluent from the anaerobic process

Although most biodegradable soluble TOC in influent could be removed by anaerobic treatment, the dark brown color and un-biodegradable components for instance lignin remained in the effluent of the anaerobic process. To treat this, the post-treatments were processed by the following methods including coagulation using NaClO and PAC, absorption by activated carbon (AC), NF, and RO membrane technology for effluent from an anaerobic digester. Two kinds of commercial membranes, NF (NTR-729HF, Nitto, Japan) and low-pressure RO (NTR-759HR, Nitto, Japan), were used to remove un-biodegradable materials and color in the effluent of the FBR. The membrane modules had an effective surface area of 60 cm<sup>2</sup> with a recycling speed of 0.15 m/s. The pressure was maintained at 0.5 MPa during the 12 h operation time and the influent concentrations were kept consistently since enough influent volume was prepared to compare permeate volume.

To remove the lignin, the main un-biodegradable material in the liquid, NaClO as an oxidizer could modify the electronic distribution on lignin surface layer that can enhance

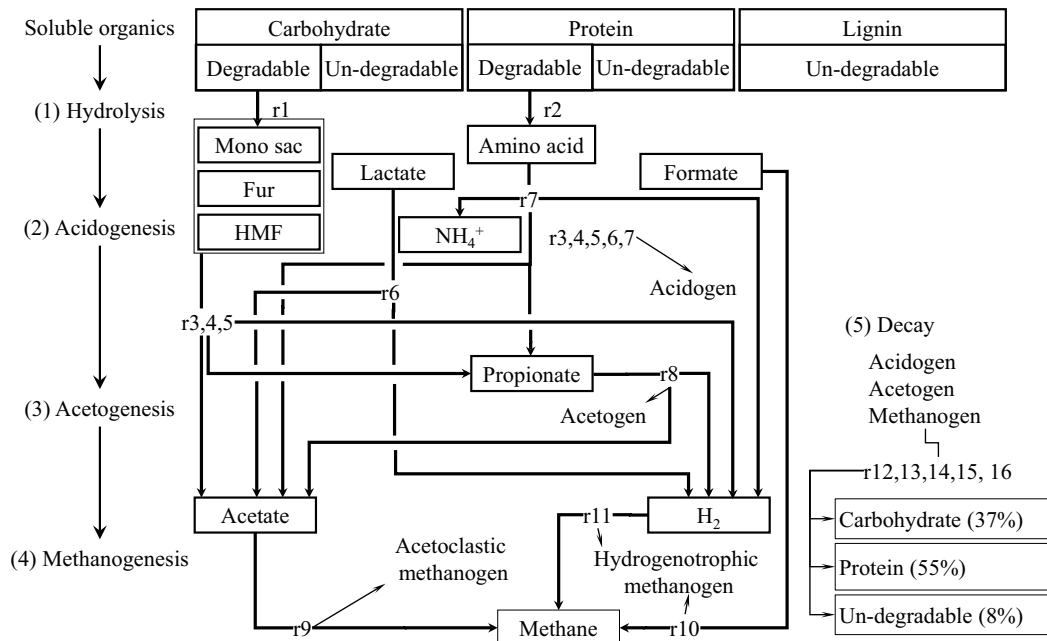


Fig. 3. Anaerobic biological reaction map for the steam explosion wastewater organics.

coagulation effect with PAC due to the macromolecule polymer formed by the electronic binding force ( $\text{ClO}^-$  and  $\text{Al}(\text{OH})_3$ ) (Ma et al. [43]). For post-treatment using  $\text{NaClO}$  and PAC, different dose of  $\text{NaClO}$  (0.5, 2, and 5 mg/L) was added into the neutralized effluent at pH 7 using 2 mol/L HCl for oxidizing, then PAC (0, 50, 100, and 200 mg-PAC/L) was added and neutralization was operated for after PAC addition.

For post-treatment using AC, the AC (WG465, Kurita Water Industries Ltd., Japan) was crushed and sieved using a 355  $\mu\text{m}$  aperture net. The effluent from the anaerobic process was added to AC and kept at 35°C temperature control chamber, stirring at 200 rpm for 24 ho, treatment time was decided by preliminary tests, which adsorption consequent could be equilibrium in 1 d approximately, then the treated water was centrifuged (10,000 rpm, 5 min) for supernatant analysis on TOC and color. The experimental data were fitted to the Freundlich equation, which is the most common model for describing the AC equilibrium [34] as shown in the following equation.

$$\log(Q_{\text{ads}}) = \log(K_F) + \frac{1}{n} \log(C_e) \quad (1)$$

where  $Q_{\text{ads}}$  is the adsorption capacity at the equilibrium concentration,  $K_F$  is the Freundlich concentration,  $C_e$  is the equilibrium concentration,  $n$  is the homogeneity factor of the Freundlich equation.

To determine the fit goodness of experimental values, the coefficient of determination ( $r^2$ ) and the average relative error ( $P$ ) were calculated. The  $P$ -value is defined as:

$$P = \left( \frac{100}{N} \right) \sum \left( \frac{|Q_{\text{ads}(\text{exp})} - Q_{\text{ads}(\text{pred})}|}{Q_{\text{ads}(\text{exp})}} \right) \quad (2)$$

where  $Q_{\text{ads}(\text{exp})}$  is the experimental adsorption capacity,  $Q_{\text{ads}(\text{pred})}$  is the predicted adsorption capacity at equilibrium concentration ( $C_e$ ) according to the equation under study with the best-fitted parameters,  $N$  the number of experimental data. The lower the  $P$ -value, the better is the fit.

### 3. Results and discussion

#### 3.1. Composition of the SEWW

The characterizations of 3 times' collected SEWW samples used for the influent of continuous anaerobic digestion experiment are shown in Table 3. In general, the wastewater was acidic with pH in the range of 2.6–3.0. This wastewater also contained high COD (more than 21,000 mg-COD/L) and TOC concentrations (8,784–9,684 mg-C/L), strong odor, and dark brown color which mainly comes from high lignin concentration (5,521–6,929 mg/L). Carbohydrate (8,070–13,642 mg/L) contributed significantly to the compositions of the SEWW while protein (581–691 mg/L), sugar derivatives (furfural: 510–1,743 mg/L and hydroxyl-methyl-furfural: 544–1,129 mg/L) and low-molecule fatty acids (formate: 700–1,529 mg/L, acetate: 797–1,597 mg/L, lactate: 412–1,687 mg/L, oxalate: 70–156 mg/L, propionate: 0–45 mg/L, butyrate: 0–52 mg/L) was detected. Total nitrogen (175–209 mg/L), total phosphorus (21–31 mg/L), ammonium nitrogen (5.5–7.4 mg/L), and inorganic cations/anions ( $\text{Na}^+$ ,  $\text{K}^+$ ,  $\text{Ca}^{2+}$ ,  $\text{Mg}^{2+}$ ,  $\text{Cl}^-$ ,  $\text{SO}_4^{2-}$ ) were also measured to detect the constituents of the wastewater, but these concentrations were not significant as listed and shown in Table 3.

#### 3.2. Anaerobic digestion process

The methane production rate and calculated methane conversion efficiency were plotted as shown in Fig. 4a. The initial VLR was 4.46 kg-COD/ $\text{m}^3/\text{d}$  and incrementally

Table 1  
Process rates in the anaerobic degradation of steam explosion wastewater

	Process	Rate expression
$r_1$	Hydrolysis of carbohydrate	$k_{h,ca} \cdot \left( \frac{S_{ca}}{K_{X,ca} \cdot X_{B,ca} + S_{ca}} \right) \cdot X_{B,ca}$
$r_2$	Hydrolysis of protein	$k_{h,pr} \cdot \left( \frac{S_{pr}}{K_{X,pr} \cdot X_{B,pr} + S_{pr}} \right) \cdot X_{B,pr}$
$r_3$	Uptake of monosaccharide	$\mu_{max,su} \cdot \left( \frac{S_{su}}{K_{S,su} + S_{su}} \right) \cdot \left( \frac{S_{su}}{S_{su} + S_{fur} + S_{hmf} + S_{lac}} \right) X_{B,su}$
$r_4$	Uptake of furfural	$\mu_{max,fur} \cdot \left( \frac{S_{fur}}{K_{S,fur} + S_{fur}} \right) \cdot \left( \frac{S_{fur}}{S_{su} + S_{fur} + S_{hmf} + S_{lac}} \right) X_{B,fur}$
$r_5$	Uptake of HMF	$\mu_{max,hmf} \cdot \left( \frac{S_{hmf}}{K_{S,hmf} + S_{hmf}} \right) \cdot \left( \frac{S_{hmf}}{S_{su} + S_{fur} + S_{hmf} + S_{lac}} \right) X_{B,hmf}$
$r_6$	Uptake of lactate	$\mu_{max,lac} \cdot \left( \frac{S_{lac}}{K_{S,lac} + S_{lac}} \right) \cdot \left( \frac{S_{lac}}{S_{su} + S_{fur} + S_{hmf} + S_{lac}} \right) X_{B,lac}$
$r_7$	Uptake of amino acid	$\mu_{max,aa} \cdot \left( \frac{S_{aa}}{K_{S,aa} + S_{aa}} \right) \cdot X_{B,aa}$
$r_8$	Uptake of propionate	$\mu_{max,pro} \cdot \left( \frac{S_{pro}}{K_{S,pro} + S_{pro}} \right) \cdot \left( \frac{K_{I,pro}^n}{K_{I,pro}^n + S_{pro}^n} \right) \cdot X_{B,pro}$
$r_9$	Uptake of acetate	$\mu_{max,ace} \cdot \left( \frac{S_{ace}}{K_{S,ace} + S_{ace}} \right) \cdot X_{B,ace}$
$r_{10}$	Uptake of formate	$\mu_{max,for} \cdot \left( \frac{S_{for}}{K_{S,for} + S_{for}} \right) \cdot X_{B,for}$
$r_{11}$	Uptake of hydrogen	$\mu_{max,hyd} \cdot \left( \frac{S_{hyd}}{K_{S,hyd} + S_{hyd}} \right) \cdot X_{B,hyd}$
$r_{12}$	Decay of sugar degrader	$b_{su} \cdot X_{B,su}$
$r_{13}$	Decay of amino acid degrader	$b_{aa} \cdot X_{B,aa}$
$r_{14}$	Decay of propionate degrader	$b_{pro} \cdot X_{B,pro}$
$r_{15}$	Decay of acetate utilizer	$b_{ace} \cdot X_{B,ace}$
$r_{16}$	Decay of hydrogen utilizer	$b_{hyd} \cdot X_{B,hyd}$

Table 2  
List of initial biomass concentrations for simulation

Microorganisms	Concentration (mg-COD/L)
Sugar degrader (acidogen)	400
Amino acid degrader (acidogen)	400
Propionate degrader (acetogen)	300
Acetate utilizer (methanogen)	340
Hydrogen utilizer (methanogen)	300

increased to 10.94 kg-COD/m<sup>3</sup>/d during 160 d of operation. The methane production rate correspondingly changed with VLR. That indicated that some organics in the influent were biodegraded and converted into methane gas. The methane production rate was simulated reasonably from influent VLR and constructed models. As shown in Fig. 4b, about 50% of the SEWW COD was converted to methane, and it can be estimated that half of influent COD was un-biodegradable material or different to be biodegraded, which main contents were predicted to lignin, cellulose, hemicellulose, and some productions from Maillard reaction, these material needed

Table 3  
Constituents of the steam explosion wastewater

Parameter unit: mg/L except pH	COD factor	Steam explosion wastewater		
		Sample 1 (day 0–66)	Sample 2 (day 67–107, 143–160)	Sample 3 (day 108–142)
pH		2.61	2.87	3.03
Total solid		17,419	18,347	17,073
Total volatile solid		17,000	17,900	16,700
COD		24,100	26,250	21,390
TOC		8,784	9,684	9,375
Carbohydrate	1.07	9,825	8,070	13,642
Protein	1.4	581	650	691
Lignin	1.87	6,020	5,521	6,929
Furfural	1.67	510	689	1,743
Hydroxyl-methyl-furfural	1.52	1,009	1,129	544
Formate	0.35	1,294	1,529	700
Acetate	1.07	1,583	1,597	797
Lactate	1.07	1,687	732	412
Oxalate	0.18	107	70	156
Propionate	1.51	ND	45	15
Butyrate	1.82	ND	ND	52
Total nitrogen		175	196	209
Total phosphorus		30	31	21
Ammonium nitrogen		5.5	6.5	7.4
Na <sup>+</sup>		113	99	145
K <sup>+</sup>		42	40	23
Ca <sup>2+</sup>		87	77	76
Mg <sup>2+</sup>		40	38	28
Cl <sup>-</sup>		21	18	8
SO <sub>4</sub> <sup>2-</sup>		80	111	87
Acid-insoluble materials (assumed to be silicate)		316	305	259

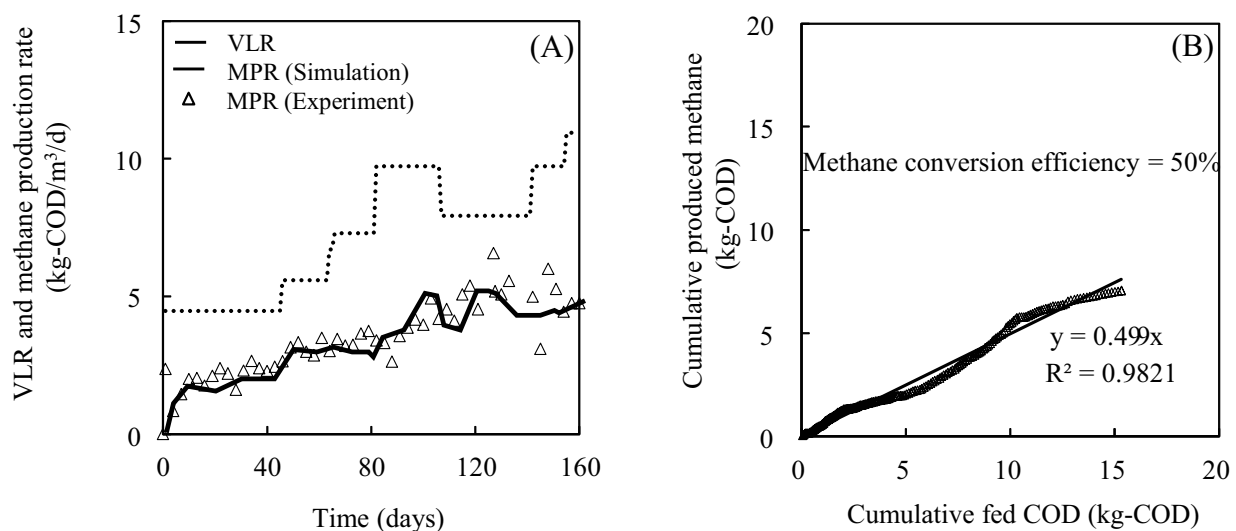


Fig. 4. Volumetric loading rate, CH<sub>4</sub> production rate and CH<sub>4</sub> conversion efficiency.

to treat by post-treatment after the anaerobic digestion process.

During the operation soluble TOC concentration was in the range of 2,300–4,400 mg-C/L while SS fluctuated from 100 to 300 mg/L in the effluent of the FBR shown in Fig. 5, which was attributed to the un-biodegradable particulate in raw wastewater and detached biofilm from the reactor. According to the soluble TOC influent and effluent, the removal efficiency corresponded to the change of VLR with an average value of 64%. The response of soluble TOC concentrations and SS concentrations in the effluent were reasonably simulated as shown in the figure.

The soluble effluent constituents (plots) in terms of carbohydrate, protein, propionate, acetate, lignin, and ammonium nitrogen were summarized in Fig. 6 together with the simulation results (solid lines). Comparing the total carbohydrate concentration in the influent, around 713 mg-COD/L of un-biodegradable organics were retained in the reactor indicating that almost all of the carbohydrate was degraded. Approximately 33% of the un-biodegradable protein (293 mg-COD/L) was retained during 160 d of operation. One of the reasons for detected remained carbohydrate and protein compounds in the anaerobic reactor were predicted to production from the Maillard reaction since the carbohydrate and protein (or amino acids) existed in the liquid from the steam explosion pretreatments, which support materials for Maillard reaction [35,36]. Although the Maillard reaction was generally considered to occur from around 140°C–165°C, many recipes called for an oven temperature high enough to ensure that a Maillard reaction occurs [37], thus in 230°C pretreatment process the occurrence of Maillard reaction became possible. Since Maillard reaction productions were the un-biodegradable materials with similar structures of carbohydrate and protein, when carbohydrate and protein analysis methods were utilized, Maillard reaction productions were included in detected results, which were considered as un-biodegradable carbohydrate and protein. In addition, soluble lignin was not degraded throughout

the experimental period and considered as the soluble inert. The ammonia nitrogen produced from the protein decomposition was 3.5–7 mg-N/L and was considered to be a low concentration. From day 83, when the VLR was increased to 9.72 kg-COD/m<sup>3</sup>/d, the measured propionate concentration in the reactor was 1,940 mg-COD/L (Fig. 6) on day 100. The VLR was reduced to 7.92 kg-COD/m<sup>3</sup>/d at day 108 leading to a decline in propionate concentration to 1,280 mg-COD/L. After that propionate increased again from day 120 and reached 2,300 mg-COD/L with short-time VLR increasing (not shown in Fig. 3). Despite the high concentration of propionate, the acetate concentration was stable in the range of 100–250 mg-COD/L in the reactor.

### 3.3. Simulation and kinetic parameters

The datasets for CH<sub>4</sub> production rate, effluent soluble TOC and SS concentrations, carbohydrate, protein, lignin, propionate, acetate, and ammonia concentrations in Figs. 4–6 were simulated reasonably (solid line) for the FBR using the constructed model and influent concentrations. In the simulation process, high half-saturation coefficients ( $K_s$ ) of process rates were used. Since a high  $K_s$  was applied the role of the biofilm process in the FBR was integrated. Nevertheless, almost all kinetic parameters for individual organics in SEWW were calibrated based on the results of the batch test and are listed in Table 4. Comparing to the default values [31,32,38–41], the kinetics were in a reasonable range. However, the maximum specific uptake rates of propionate (21.5 d<sup>-1</sup>) and acetate (10 d<sup>-1</sup>) were remarkably higher than that adapted from ADM1 (0.02–1.07 d<sup>-1</sup> for propionate and 0.02–1.4 d<sup>-1</sup> for acetate) [29]. The concentration of the propionate degrader was obtained focusing on the reaction rate of the hydrogenotrophic methanogenic biomass, formate, and propionate concentrations in the reactor. To express the hydrogen inhibition for the propionate degrader, a pair of  $K_i = 0.003$  mg-COD/L and  $n = 0.118$  was applied. The simulation was highly sensitive to changes in  $K_i$  resulting in a minor error in simulated and measured

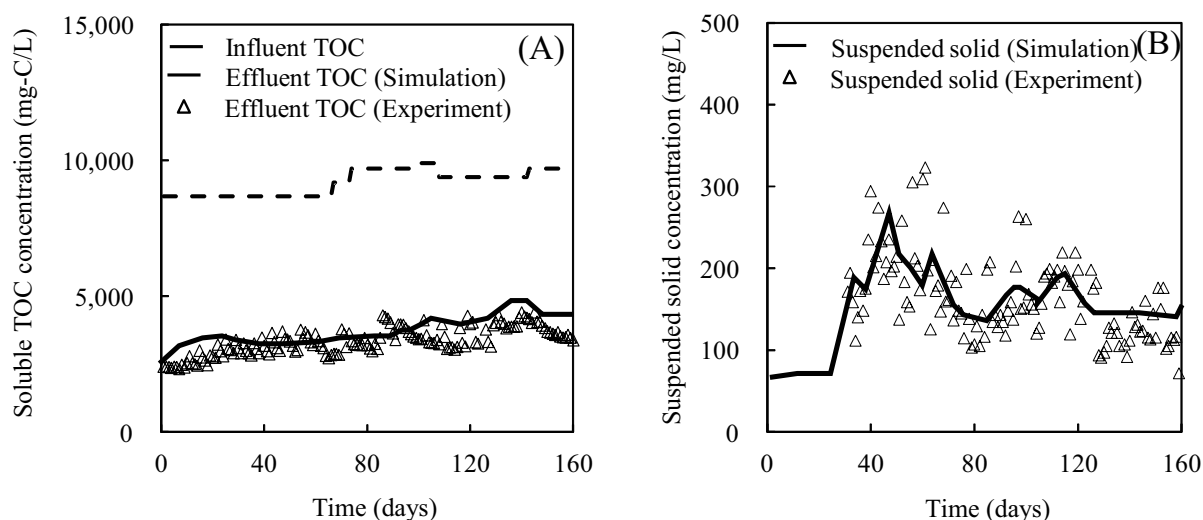


Fig. 5. Soluble TOC and SS concentration.

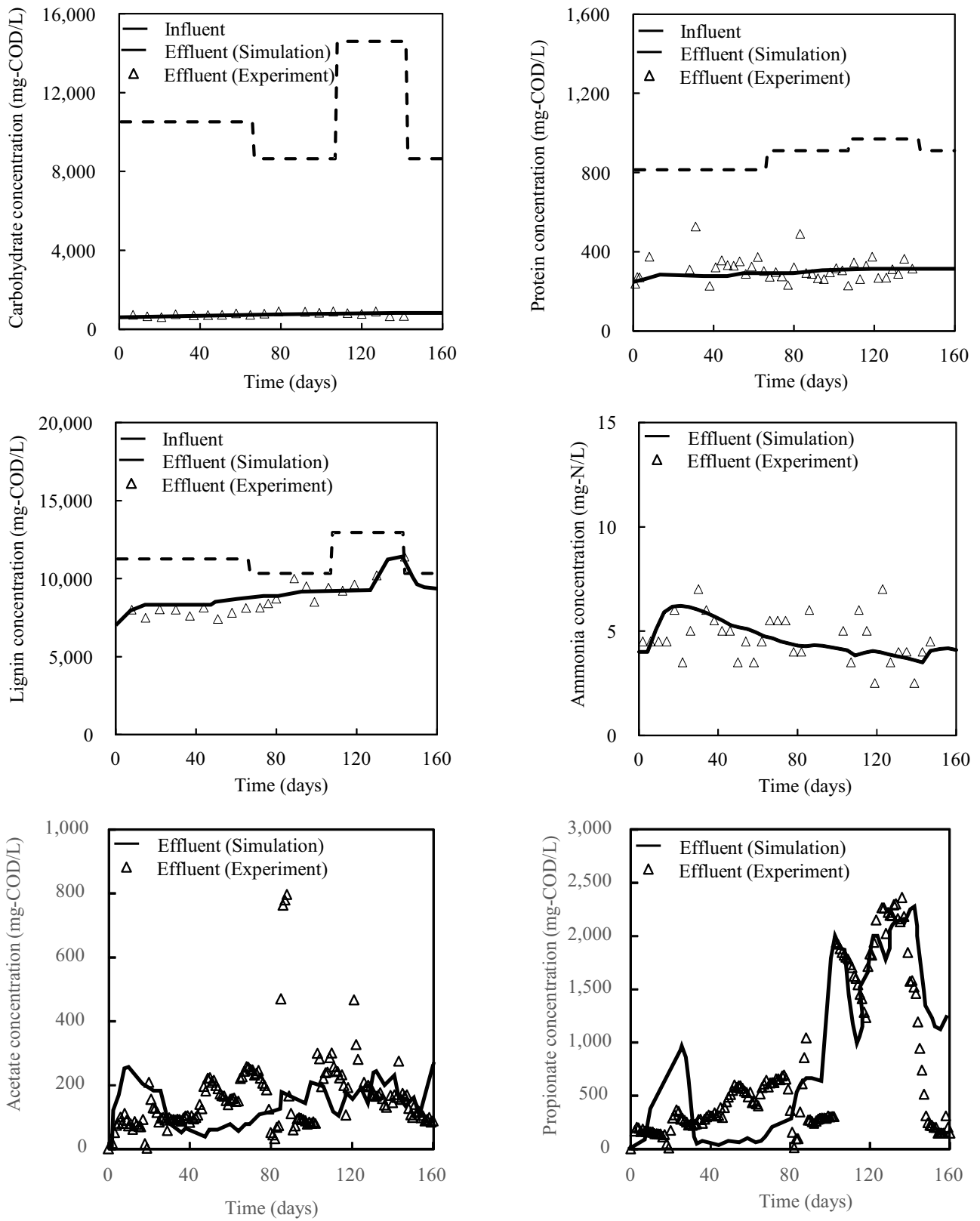


Fig. 6. Compositions in the effluent.

Table 4  
List of kinetics for anaerobic degradation from steam explosion wastewater

Symbol	Expression	Value (this study)	Value (references)	Unit
$k_{h,ca}$	Maximum specific hydrolysis rate on carbohydrate	10	1.25–18 [21,28]	$d^{-1}$
$K_{X,ca}$	Half-saturation coefficient for carbohydrate hydrolysis	8	0.5–22.5 [28,29]	mg-COD/L
$k_{h,pr}$	Maximum specific hydrolysis rate on protein	4	1.04–18 [29,30]	$d^{-1}$
$K_{X,pr}$	Half-saturation coefficient for protein hydrolysis	15	0.26–22.5 [28,29]	mg-COD/L
$\mu_{max,su}$	Maximum specific growth rate from carbohydrate	3	0.41–21 [31]	$d^{-1}$
$K_{s,su}$	Half-saturation coefficient on carbohydrate	250	3–90 [31]	mg-COD/L
$\mu_{max,fur}$	Maximum specific growth rate from furfural	10	Nil	$d^{-1}$
$K_{s,fur}$	Half-saturation coefficient on furfural	250	Nil	mg-COD/L
$\mu_{max,hmf}$	Maximum specific growth rate from HMF	10	Nil	$d^{-1}$
$K_{s,hmf}$	Half-saturation coefficient on HMF	250	Nil	mg-COD/L
$\mu_{max,lac}$	Maximum specific growth rate from lactate	10	Nil	$d^{-1}$
$K_{s,lac}$	Half-saturation coefficient on lactate	250	Nil	mg-COD/L
$\mu_{max,aa}$	Maximum specific growth rate from the amino acid	2	2.36–4 [31]	$d^{-1}$
$K_{s,aa}$	Half-saturation coefficient on amino acid	100	7.5–70 [31]	mg-COD/L
$\mu_{max,pro}$	Maximum specific growth rate from propionate	21.5	0.02–1.07 [31]	$d^{-1}$
$K_{s,pro}$	Half-saturation coefficient on propionate	110	1–57 [31]	mg-COD/L
$K_{I,pro}$	Inhibition coefficient from hydrogen	0.003	0.001–0.008 [31]	mg-COD/L
$n$	Power factor	0.118	2 [29]	–
$\mu_{max,ace}$	Maximum specific growth rate from acetate	10	0.02–1.41 [31]	$d^{-1}$
$K_{s,ace}$	Half-saturation coefficient on acetate	300	0.2–71 [31]	mg-COD/L
$\mu_{max,for}$	Maximum specific growth rate from formate	12	Nil	$d^{-1}$
$K_{s,for}$	Half-saturation coefficient on formate	250	Nil	mg-COD/L
$\mu_{max,hyd}$	Maximum specific growth rate from hydrogen	3.4	0.02–12 [31]	$d^{-1}$
$K_{s,hyd}$	Half-saturation coefficient on hydrogen	1	1 [30]	mg-COD/L
$b_{su}$	Decay rate of sugar degrader	0.01	0.02–0.8 [30,31]	$d^{-1}$
$b_{aa}$	Decay rate of amino acid degrader	0.01	0.02–0.8 [30,31]	$d^{-1}$
$b_{pro}$	Decay rate of propionate degrader	0.01	0.01–0.2 [30,31]	$d^{-1}$
$b_{ace}$	Decay rate of acetate utilizer	0.01	0.01–0.05 [30,31]	$d^{-1}$
$b_{hyd}$	Decay rate of hydrogen utilizer	0.01	0.009–0.3 [30,31]	$d^{-1}$

Nil: non-value

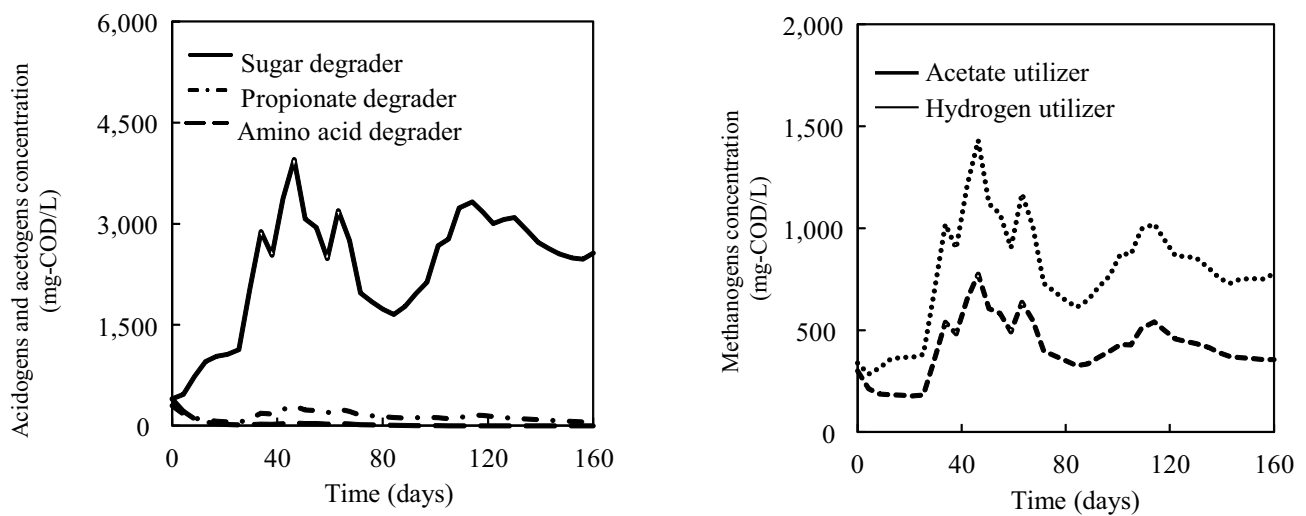


Fig. 7. Calculated active biomass concentrations.

values of propionate as shown in Fig. 6. And the obtained kinetics  $K_{i,pro}$  and some half-saturation coefficient values in this system were different from previous UASB research [2], which reason was surmised to carrier media biofilm reactor's sensitivity difference.

The dynamic change for acidogens (sugar and amino acid degraders), acetogens (syntrophic propionate degrader), and methanogens (acetate and hydrogen utilizers) were calculated as shown in Fig. 7. Sugar degraders remained in the reactor at high concentration while amino acid and propionate degraders decreased quickly because carbohydrate concentration in influent for the anaerobic process was much higher (12.4–19.7 times) than protein that is shown in Table 3, resulting in the difference of corresponding substrate utilizers (sugar degrader, propionate degrader, and amino acid degrader) shown in the left side of Fig. 7. The two estimated kinds of active methanogens were stable in the reactor because influent CODs and compositions for three times were almost in the same level as shown in Table 3, as the final COD utilizers (acetate utilizer and hydrogen utilizer) for methane fermentation, the biomass amount should be at a stable level.

To predict the  $CH_4$  conversion efficiency at different VLRs the simulations at steady state conditions were conducted. As shown in Table 5 stabilized methane conversion efficiency (45%–50%) at the VLR from 4.46–9.72 kg-COD/ $m^3/d$  was obtained. Even when a high OLR (9.72 kg-COD/ $m^3/d$ ) was applied, 45% of COD was converted to methane with soluble COD and soluble TOC concentrations in the effluent of 11,120 mg-COD/L and 3,604 mg-C/L, respectively.

### 3.4. Post-treatment for un-biodegradable materials and color

A significant soluble TOC removal efficiency of approximately 64% could be obtained after biological anaerobic treatment. However a high lignin concentration and dark brown color (soluble TOC of 2,675 mg-C/L and color of 12,642 unit) remained in the effluent, and lignin was considered as the main reason of high COD and dark color [42]. In an effort to remove the TOC and color from the effluent of the FBR, oxidation combining coagulation using NaClO and PAC was conducted. The TOC and color removal efficiency was slight and neglected using single PAC addition. After oxidation by NaClO, with the PAC addition dose increasing, the TOC and color removal ratios were increased accordingly as shown in Figs. 8a and b, with 5 mg-NaClO/L and 200 mg- $Al_2O_3/L$ , TOC, and color removal ratio could be achieved at 61.6% and 70.6%. As an oxidation reagent, NaClO addition affected the TOC removal ratio

revealing the importance of oxidation in the coagulation process, which the same conclusion was also highlighted in Ma et al. [43]. According to the experimental results of 50 mg- $Al_2O_3-Al/L$  addition with different NaClO concentrations shown in Fig. 8b, the color removal ratio could be improved by increasing of NaClO addition. While in the 100 and 200 mg- $Al_2O_3/L$  additional sets in Fig. 8b, whatever the amount of NaClO addition at 0.5, 2, and 5 mg/L, there was no significant difference in color removal ratio. And comparing to results in Fig. 8a the conclusion could be obtained that the TOC removal ratio is not proportional to color in this test, which is the same experimental results with Töre [44]. One of the reasons could be predicted that the dark color from long-chain/high molecule lignin and production of Maillard reaction (for instance, melanoidins), lignin is a kind of an aromaticity macromolecule material with a ball structure form generally, the OH radical produced by NaClO could oxidize low bond energy groups in the surface of lignin structure, for instance, hydroxyl and aldehyde groups that can promote the TOC removal process with PAC coagulation. Anyway, according to the melanoidins structure [45], it cannot be oxidized and coagulated by NaClO and PAC addition, resulting in the TOC and color removal was not synchronous beyond 50 mg- $Al_2O_3/L$  addition.

As a common physical absorbance material, AC was also tested to treat effluent from the fixed-bed anaerobic reactor [46,47]. The relationship between AC addition and TOC and color removal is shown in Figs. 8c and d. The adsorption for TOC and color was fitted with the Freundlich isotherm model, the goodness of fit was evaluated by  $r^2$  and average relative error ( $P$ ) shown in Table 6.

For NF and RO post-treatment, because the permeate flux was slow at 8.06 L/ $m^2$  h (NF) and 2.83 L/ $m^2$  h (RO) respectively in the initial 24 h, the operation was discontinued after 1 d. According to TOC and color of before and after treatment with NF and RO membrane, soluble TOC and color removal efficiencies of NF were 84.2% and 96.1% respectively in the permeate, while the soluble TOC and color removal efficiencies by RO were 97.3% and 99.2% respectively as shown in the right side of Fig. 8. The

Table 6  
Equilibrium model fitting parameters for AC at 25°C

	$K_f$	$n$	$R^2$	$P$
TOC adsorption	1.06	1.3	0.986	3.68
Color adsorption	20	2.5	0.949	13.43

Table 5  
 $CH_4$  conversion efficiency at different VLR in steady-state condition

#	VLR (kg-COD/ $m^3/d$ )	S-COD <sub>eff</sub> (mg-COD/L)	S-TOC <sub>eff</sub> (mg-C/L)	$CH_4$ (kg-COD/ $m^3/d$ )	$CH_4$ conversion efficiency (%)
1	4.46	9,571	3,243	2.23	50
2	5.58	10,190	3,377	2.75	49
3	7.29	10,350	3,449	3.36	46
4	9.72	11,120	3,604	4.37	45

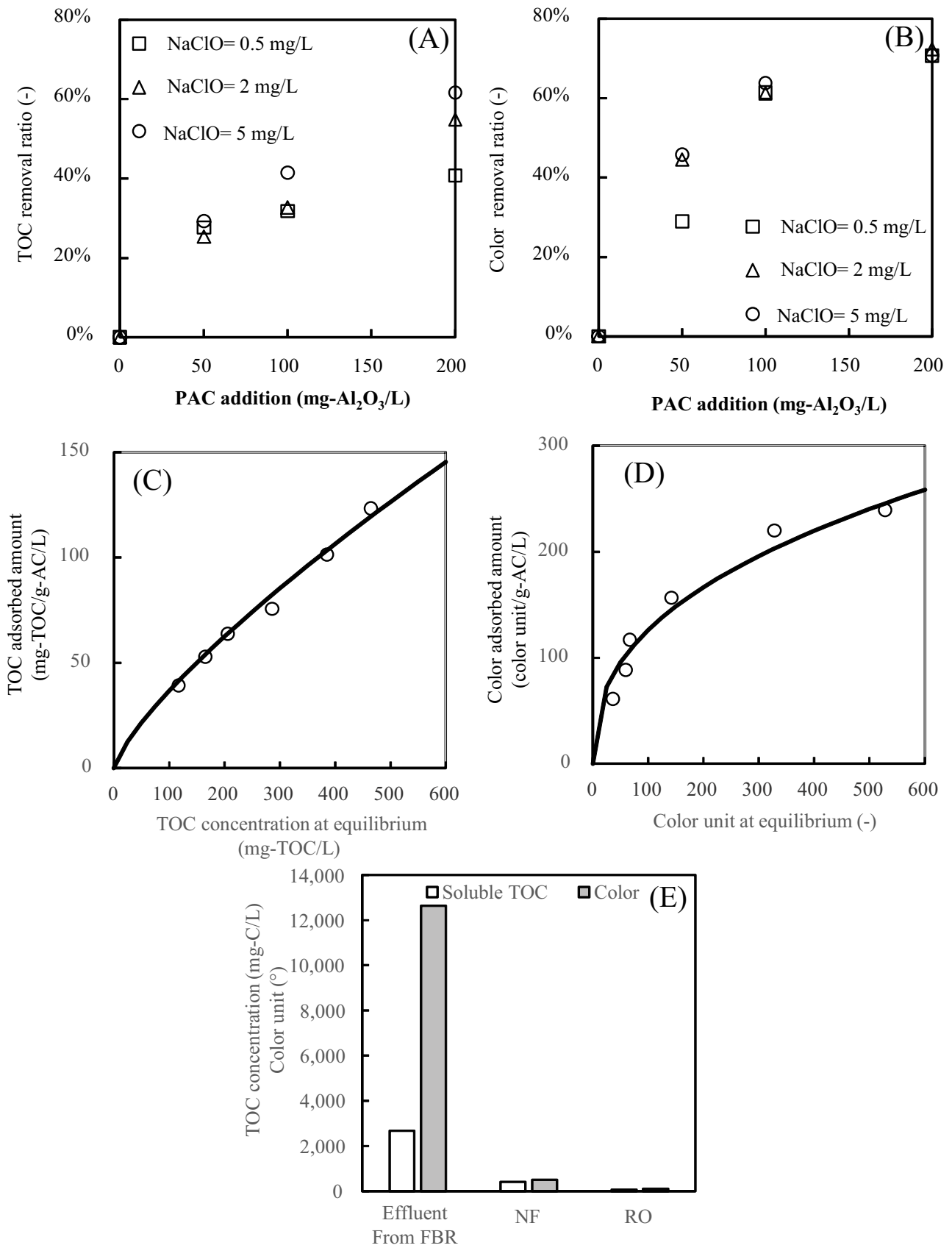


Fig. 8. Post-treatment of effluent from the fixed-bed anaerobic reactor.

RO post-treatment had a higher TOC and color removal ratio comparing the NF, while its flux was 3 times lower than NF post-treatment.

According to the experimental results from the above operation, although the physicochemical methods removed almost all of the un-biodegradable materials and color, the first test consumed a large number of chemicals (NaClO and PAC) while RO and NF membranes required much more energy for operation. Therefore, the physicochemical and membrane (RO and NF) methods for post-treatment should be employed depending on different objectives and energy accounting.

#### 4. Conclusions

In this study, a newly anaerobic fixed-bed process was developed and applied to treat waste liquid from the steam explosion stage from a bioethanol processing plant. Most of the organics in the wastewater were supposed to be readily biodegradable except lignin. The average soluble TOC removal efficiency was 64% with a methane conversion efficiency of about 50%. A kinetic model based on a modification of ADM1 and ASMs was used to reasonably simulate the methane production, soluble TOC, SS as well as the soluble effluent constituents in terms of carbohydrate, protein, propionate, acetate, lignin, and ammonium nitrogen. The role of biofilm on digestion efficiency was considered by using a high  $K_s$  for process rates. The simulation results at steady state showed that 45% of COD was converted to methane gas at a high OLR of 9.72 kg-COD/m<sup>3</sup>/d. On the other hand, some simple tests with physicochemical methods were conducted to remove un-biodegradable materials and color from the effluent. Oxidation, coagulation/flocculation, and adsorption removed 88% of soluble TOC and 98% of color while the removal efficiencies of were 98.3% (TOC), 99.3% (color) for RO membranes, and 87.9% (TOC) and 97% (color) for NF membranes, correspondingly. According to experimental results, a selective proper process could be combined for similar wastewater treatment based on different objectives and energy accounting.

#### Acknowledgments

This work was supported by JSPS Grants-in-Aid for Scientific Research (16H04439, Japan) and Science Foundation of Shandong Jianzhu University (Grant No. XNBS1824) and Shandong Provincial Key Research and Development Program (No. 2019GSF109064).

#### References

- [1] H. Kahr, A. Jäger, C. Lanzerstorfer, Bioethanol Production from Steam Explosion Pretreated Straw, in: *Bioethanol*, IntechOpen Pub, Rijeka, 2012, pp. 153–172.
- [2] M. Tutt, T. Kikas, H. Kahr, M. Pointner, P. Kuttner, J. Olt, Using steam explosion pretreatment method for bioethanol production from floodplain meadow hay, *Int. J. Hydrogen Energy*, 12 (2014) 417–424.
- [3] M.D. Ferro, M.C. Fernandes, A.F.C. Paulino, S.O. Prozil, J. Gravitis, D.V. Evtuguin, A.M.R.B. Xavier, Bioethanol production from steam explosion pretreated and alkali extracted *Cistus ladanifer* (rockrose), *Biochem. Eng. J.*, 104 (2015) 98–105.
- [4] N. Jacquet, G. Maniet, C. Vanderghem, F. Delvigne, A. Richel, Application of steam explosion as pretreatment on lignocellulosic material: a review, *Ind. Eng. Chem. Res.*, 54 (2015) 2593–2598.
- [5] C.A. Cardona, J.A. Quintero, I.C. Paz, Production of bioethanol from sugarcane bagasse: status and perspectives, *Bioresour. Technol.*, 101 (2010) 4754–4766.
- [6] M.C. de Albuquerque Wanderley, C. Martín, G.J. de Moraes Rocha, E.R. Gouveia, Increase in ethanol production from sugarcane bagasse based on combined pretreatments and fed-batch enzymatic hydrolysis, *Bioresour. Technol.*, 128 (2013) 448–453.
- [7] A.R.G. da Silva, C.E. Torres Ortega, B.-G. Rong, Techno-economic analysis of different pretreatment processes for lignocellulosic-based bioethanol production, *Bioresour. Technol.*, 218 (2016) 561–570.
- [8] Y.J. Xu, J. Li, M. Zhang, D.H. Wang, Modified simultaneous saccharification and fermentation to enhance bioethanol titers and yields, *Fuel*, 215 (2018) 647–654.
- [9] P. Silva Ortiz, S. de Oliveira Jr., Exergy analysis of pretreatment processes of bioethanol production based on sugarcane bagasse, *Energy*, 76 (2014) 130–138.
- [10] T. Steinwinder, E. Gill, M. Gerhardt, *Process Design of Wastewater Treatment for the NREL Cellulosic Ethanol Model*, National Renewable Energy Laboratory, Golden, Colorado, United States, 2011.
- [11] B. Liu, V.A. Ngo, M. Terashima, H. Yasui, Anaerobic treatment of hydrothermally solubilised sugarcane bagasse and its kinetic modelling, *Bioresour. Technol.*, 234 (2017) 253–263.
- [12] Y. Zheng, J. Zhao, F.Q. Xu, Y.B. Li, Pretreatment of lignocellulosic biomass for enhanced biogas production, *Prog. Energy Combust.*, 42 (2014) 35–53.
- [13] B. Ráduly, L. Gyenge, Sz. Szilveszter, A. Kedves, S. Crognale, Treatment of corn ethanol distillery wastewater using two-stage anaerobic digestion, *Water Sci. Technol.*, 74 (2016) 431–437.
- [14] H.H. Ngo, M.A. Khan, W.S. Guo, A. Pandey, D.-J. Lee, *Non-conventional Anaerobic Bioreactors for Sustainable Wastewater Treatment*, X.T. Bui, C. Chiemchaisri, T. Fujioka, S. Varjani, Eds., *Water and Wastewater Treatment Technologies*, Springer, Singapore, 2019, pp. 265–295.
- [15] V.A. Ngo, *The Treatment of Steam Explosion Wastewater Generated from Bioethanol Processing using Sugarcane Bagasse*, Doctoral Dissertation, Graduate School of Environmental Engineering, The University of Kitakyushu, Fukuoka-ken, Kyushu, Japan, 2016.
- [16] S. Greses, E. Tomás-Pejó, C. González-Fernández, Agroindustrial waste as a resource for volatile fatty acids production via anaerobic fermentation, *Bioresour. Technol.*, 297 (2019) 122486.
- [17] M.U. Khan, B.K. Ahring, Lignin degradation under anaerobic digestion: influence of lignin modifications—a review, *Biomass Bioenergy*, 128 (2019) 105325.
- [18] A. Silva-Teira, A. Sánchez, D. Buntner, L. Rodríguez-Hernández, J.M. Garrido, Removal of dissolved methane and nitrogen from anaerobically treated effluents at low temperature by MBR post-treatment, *Chem. Eng. J.*, 326 (2017) 970–979.
- [19] J.R. Banu, S. Kaliappan, D. Beck, High rate anaerobic treatment of Sago wastewater using HUASB with PUF as carrier, *Int. J. Environ. Sci. Technol.*, 3 (2006) 69–77.
- [20] R. Rajinikanth, R. Ganesh, R. Escudie, I. Mehrotra, P. Kumar, J.V. Thanikal, M. Torrijos, High rate anaerobic filter with floating supports for the treatment of effluents from small-scale agro-food industries, *Desal. Water Treat.*, 4 (2009) 183–190.
- [21] R. Ganesh, R. Rajinikanth, J.V. Thanikal, R.A. Ramanujam, M. Torrijos, Anaerobic treatment of winery wastewater in fixed bed reactors, *Bioprocess. Biosyst. Eng.*, 33 (2010) 619–628.
- [22] P. Sivagurunathan, P. Anburajan, J.-H. Park, G. Kumar, H.-D. Park, S.-H. Kim, Mesophilic biogenic H<sub>2</sub> production using galactose in a fixed bed reactor, *Int. J. Hydrogen Energy*, 42 (2017) 3658–3666.
- [23] S. Ramaswami, F.M. Jalal Uddin, J. Behrendt, R. Otterpohl, High-rate nitrification of saline wastewaters using fixed-bed reactors, *J. Environ. Manage.*, 243 (2019) 444–452.

- [24] S. Bharti, S. Mukherji, S. Mukherji, Water disinfection using fixed bed reactors packed with silver nanoparticle immobilized glass capillary tubes, *Sci. Total Environ.*, 689 (2019) 991–1000.
- [25] D.J. Batstone, J. Keller, I. Angelidaki, S. Kalyuzhnyi, S. Pavlostathis, A. Rozzi, W. Sanders, H. Siegrist, V. Vavilin, The IWA anaerobic digestion model no 1 (ADM1), *Water Sci. Technol.*, 45 (2002) 65–73.
- [26] M. Henze, W. Gujer, T. Mino, M.C.M. van Loosedrecht, Activated Sludge Models ASM1, ASM2, ASM2d and ASM3, IWA Publishing, London, 2000.
- [27] M. Sillanpää, M.C. Ncibi, A. Matilainen, M. Vepsäläinen, Removal of natural organic matter in drinking water treatment by coagulation: a comprehensive review, *Chemosphere*, 190 (2018) 54–71.
- [28] APHA-AWWA-WEF, Standard Methods for the Examination of Water and Wastewater, 22nd ed., American Public Health Association/American Water Works Association/Water Environment Federation, New York, USA, 2012.
- [29] M. DuBois, K.A. Gilles, J.K. Hamilton, P.A. Rebers, F. Smith, Colorimetric method for determination of sugars and related substances, *Anal. Chem.*, 28 (1956) 350–356.
- [30] O.H. Lowry, N.J. Rosebrough, A.L. Farr, R.J. Randall, Protein measurement with the Folin phenol reagent, *J. Biol. Chem.*, 193 (1951) 265–275.
- [31] U. Satyanarayana, U. Chakrapani, *Biochemistry*, 3rd ed., Books and Allied Pvt. Ltd., Kolkata, 2006.
- [32] H.-H. King, E. Avni, R. Coughlin, P. Solomon, Modeling Tar Composition in Lignin Pyrolysis, 186th National Meeting of the American Chemical Society, Abstracts of Papers of the American Chemical Society, Washington D.C., USA, 1983.
- [33] B.L.V.A. Ngo, M. Terashima, H. Yasui, High-rate Anaerobic Treatment of Steam Explosion Wastewater from Bioethanol Process Using Sugarcane Bagasse, *Proceeding of Water and Environment Technology Conference 2016*, Tokyo, Japan, 2016.
- [34] L.H. Velazquez-Jimenez, J.A. Arcibar-Orozco, J.R. Rangel-Mendez, Overview of As(V) adsorption on Zr-functionalized activated carbon for aqueous streams remediation, *J. Environ. Manage.*, 212 (2018) 121–130.
- [35] P. Chellan, R.H. Nagaraj, Protein crosslinking by the Maillard reaction: dicarbonyl-derived imidazolium crosslinks in aging and diabetes, *Arch. Biochem. Biophys.*, 368 (1999) 98–104.
- [36] F.-L. Gu, J.M. Kim, S. Abbas, X.-M. Zhang, S.-Q. Xia, Z.-X. Chen, Structure and antioxidant activity of high molecular weight Maillard reaction products from casein–glucose, *Food Chem.*, 120 (2010) 505–511.
- [37] G.R. Waller, M.S. Feather, *The Maillard Reaction in Foods and Nutrition*, American Chemical Society, Washington D.C., USA, 1983.
- [38] V.A. Vavilin, B. Fernandez, J. Palatsi, X. Flotats, Hydrolysis kinetics in anaerobic degradation of particulate organic material: an overview, *Waste Manage.*, 28 (2008) 939–951.
- [39] V.A. Vavilin, S.V. Rytov, L.Y. Lokshina, A description of hydrolysis kinetics in anaerobic degradation of particulate organic matter, *Bioresour. Technol.*, 56 (1996) 229–237.
- [40] F. Mairet, O. Bernard, M. Ras, L. Lardon, J.-P. Steyer, Modeling anaerobic digestion of microalgae using ADM1, *Bioresour. Technol.*, 102 (2011) 6823–6829.
- [41] H. Siegrist, D. Vogt, J.L. Garcia-Heras, W. Gujer, Mathematical model for meso- and thermophilic anaerobic sewage sludge digestion, *Environ. Sci. Technol.*, 36 (2002) 1113–1123.
- [42] D. Humpert, M. Ebrahimi, P. Czermak, Membrane technology for the recovery of lignin: a review, *Membranes*, 6 (2016) 42.
- [43] P. Ma, S.L. Fu, H.M. Zhai, K. Law, C. Daneault, Influence of TEMPO-mediated oxidation on the lignin of thermomechanical pulp, *Bioresour. Technol.*, 118 (2012) 607–610.
- [44] G.Y. Töre, R. Ata, S.Ö. Çelik, Ş.K. Sesler, Colour removal from biologically treated textile dyeing wastewater with natural and novel pre-hydrolysed coagulants, *J. Turkish Chem. Soc., Section A: Chemistry*, 5 (2017) 23–36.
- [45] H.-Y. Wang, H. Qian, W.-R. Yao, Melanoidins produced by the Maillard reaction: structure and biological activity, *Food Chem.*, 128 (2011) 573–584.
- [46] S. Wong, N. Ngadi, I.M. Inuwa, O. Hassan, Recent advances in applications of activated carbon from biowaste for wastewater treatment: a short review, *J. Cleaner Prod.*, 175 (2018) 361–375.
- [47] S. Jafarnejad, Activated sludge combined with powdered activated carbon (PACT process) for the petroleum industry wastewater treatment: a review, *Chem. Int.*, 3 (2017) 268–277.